STRESS SINGULARITIES IN PIEZOELECTRIC MULTI-MATERIAL SYSTEMS

W. Mayland, W. Becker
TU Darmstadt, Fachgebiet Strukturmechanik
Hochschulstr. 1, 64289 Darmstadt, Germany
mayland@mechanik.tu-darmstadt.de

SUMMARY

The scaled boundary finite element method in an extension for piezoelectric materials is used to analyze the orders of stress singularities for various two- and three-dimensional situations, proving the method to be an efficient tool for the determination of stress singularity orders for composites of linear-elastic and piezoelectric material.

Keywords: Scaled boundary finite element method, stress singularities, piezoelectric material, semi-analytical method, multi-material composites

INTRODUCTION

In the case of piezoelectric multi-material composites with geometrical and/or material discontinuities, singularities occur in the stress fields as well as in the electric fields. The criticality of the stress singularities in such situations can be assessed by the use of two essential characteristics of a stress singularity, namely the singularity exponent and the corresponding generalized stress intensity factor. While the orders of stress singularities are known for many elastostatic situations, further research is needed for piezoelectric multi-material systems. Analytical solutions rarely exist, and common numerical methods such as the finite element method can only be applied with considerable numerical effort. In this contribution, the scaled boundary finite element method in an extension for piezoelectric materials is used to analyze the orders of stress singularities for various two- and three-dimensional situations.

STRESS SINGULARITIES

Stress singularities occur in situations with material and/or geometric discontinuities within the scope of linear elasticity theory, for example at cracks and notches or material interfaces at a free edge. While stress singularities are of theoretical nature, at the same time they are a good indicator of weak locations in structures and can be used to assess the criticality of a given situation to avoid failure.

When stress singularities occur, using a spherical coordinate system r, φ_1, φ_2 the asymptotic local displacement and stress fields can be represented in the following form (where the singularity is placed at $r=0$, see Fig. 1):

$$u_i = \sum_{m=1}^{\infty} K_m r^{\lambda_m} g_{im}(\varphi_1, \varphi_2) \quad , \quad \sigma_{ij} = \sum_{m=1}^{\infty} K_m r^{\lambda_m - 1} f_{ijm}(\varphi_1, \varphi_2)$$

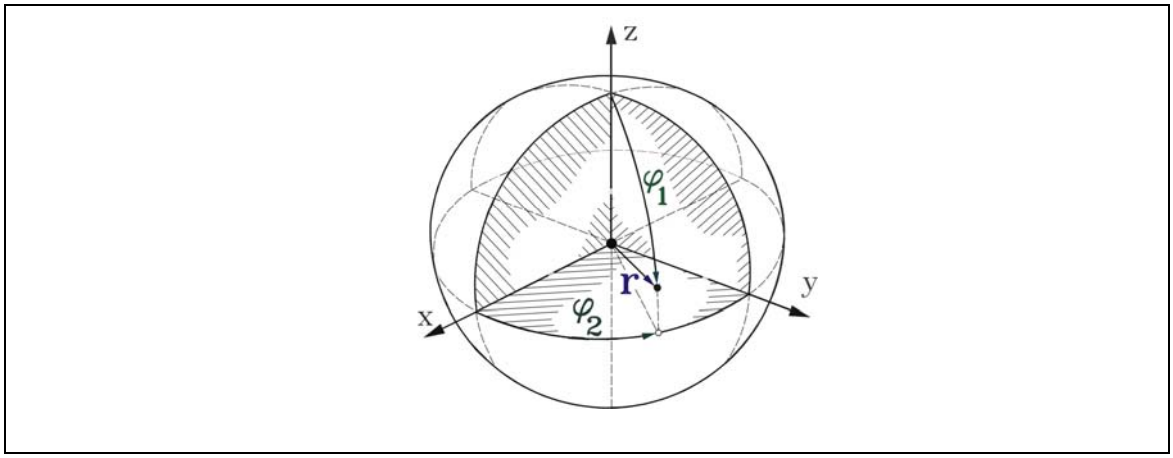

Figure 1: Spherical coordinate system.

Herein an exponential dependence is assumed in radial direction, while the functions g_{im} and f_{ijm} represent the angular variation. The stress singularities are characterized by the generalized stress intensity factors K_m as well as the singularity exponents or orders, that generally are complex numbers of the form ($Re\ \lambda_m$-1, $Im\ \lambda_m$). Singular stresses occur when $0 > Re\ \lambda_m - 1 > -1$. A well-known example is the singularity occurring at a crack tip, where $\sigma_{ij} \sim r^{-0.5}$. The orders of stress singularities are known for many elastostatic cases, but are still unknown for various geometrical situations and material combinations for elastic and piezoelectric multi-material systems. Since analytical solutions do not generally exist, and standard numerical methods such as the finite element method usually require considerable effort or can sometimes not be used at all to determine stress singularity orders, the scaled boundary finite element method is chosen for the analysis in this contribution.

THE SCALED BOUNDARY FINITE ELEMENT METHOD

The scaled boundary finite element method is a semi-analytical method combining the advantages of the boundary element method and the finite element method. The method, developed by Wolf and Song [1,2] and extended for piezoelectric material behaviour by Artel and Becker [3], requires geometric similarity of the analyzed structure in the sense of being scalable with respect to a discrete point, the so-called similarity center. It can be applied to any anisotropic linear-elastic material behaviour. Whereas in the scaling direction a closed-form analytical representation is chosen for all relevant field quantities, the method employs a finite element discretization along the boundary or in the circumferential direction. Correspondingly, this approach can be considered a semi-analytical method. Since the behaviour in the scaling direction is obtained as the analytical solution of a system of ordinary differential equations, the discretization effort is reduced by one dimension and only the boundary needs to be discretized. On the other hand, in contrast to the boundary element method, the scaled

boundary finite element method does not require a fundamental solution and thus is more widely applicable. Compared to the finite element method, the effort required for results of comparable quality is significantly lower.

Singularity orders can be obtained with little effort and high precision by this method if the similarity center is placed directly at the location of the singularity. The scaled boundary finite element method can be applied to various situations where other methods do not apply, and it generally requires less computational effort than other methods (e.g. finite element method) for the determination of stress singularity orders. This is due to the reduction of the problem dimension mentioned above as well as the fact that existent singularities are inherently taken into account by the underlying series representation of the asymptotic field quantities. As a consequence, a rather coarse mesh yields very accurate results at the similarity center where other methods require a very fine discretization to capture the singularity at all.

For piezoelectric behavior the standard material equations read

$$\boldsymbol{\sigma} = \mathbf{C}\boldsymbol{\varepsilon} - \mathbf{e}^T\mathbf{E} \quad , \quad \mathbf{D} = \mathbf{e}\boldsymbol{\varepsilon} + \epsilon\mathbf{E}$$

where **σ** denotes the stress tensor, **ε** the strain tensor, **C** the mechanical stiffness matrix, **D** the electric flux vector, **E** the electric field strength vector, **e** the piezoelectric coupling matrix, and ϵ the dielectrical matrix. The elastostatic and electrostatic equilibrium conditions are

$$\sigma_{i1,1} + \sigma_{i2,2} + \sigma_{i3,3} + f_i = 0 \quad , \qquad D_{i1,1} + D_{i2,2} + D_{i3,3} - q = 0 \quad , \quad i = 1,2,3$$

where f_i are the mechanical body force components and q is the electric body charge. Together with the geometrically linear kinematic equations as well as the representation of the electric field strength through the electric potential φ

$$\varepsilon_{ij} = \frac{1}{2}\left(u_{i,j} + u_{j,i}\right) \quad , \qquad E_i = -\varphi_{,i} \quad , \quad i = 1,2,3$$

this leads to the following weak form of the equilibrium

$$\int_\Omega \left(\boldsymbol{\varepsilon}^T\mathbf{C} - \mathbf{E}^T\mathbf{e}\right)\delta\boldsymbol{\varepsilon}\, d\Omega = \int_\Omega \mathbf{f}\delta\mathbf{u}\, d\Omega + \int_\Gamma \mathbf{t}\delta\mathbf{u}\, d\Gamma$$

$$\int_\Omega \left(\boldsymbol{\varepsilon}^T\mathbf{e} + \mathbf{E}^T\epsilon\right)\delta\mathbf{E}\, d\Omega = \int_\Omega \mathbf{q}\delta\varphi\, d\Omega + \int_\Gamma \mathbf{Q}\delta\varphi\, d\Gamma$$

Introducing the scaled boundary coordinates ξ in scaling direction and η and ζ on the boundary Γ (see Fig. 2 for the two-dimensional case with ξ and η) and representing the boundary by a set of points (x_0+x_S), (y_0+y_S), and (z_0+z_S), the coordinates of a point inside the domain can be transformed from a Cartesian coordinate system as follows

$$\begin{aligned} x &= x_0 + \xi x_S(\eta,\zeta) \\ y &= y_0 + \xi y_S(\eta,\zeta) \\ z &= z_0 + \xi z_S(\eta,\zeta) \end{aligned}$$

where (x_0,y_0,z_0) are the coordinates of the similarity center and ξ is the normalized scaling factor in radial direction.

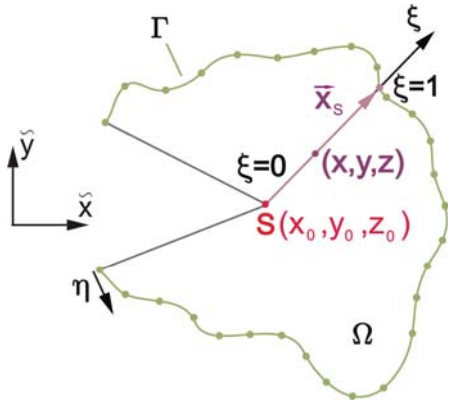

Figure 2: Scaled boundary coordinates.

Discretizing the boundary, the geometry can be represented with the help of shape functions **h** and the vectors **x**, **y**, **z** of nodal coordinates as follows

$$\begin{aligned} x &= x_0 + \xi \mathbf{h}^T(\eta,\zeta)\mathbf{x} \\ y &= y_0 + \xi \mathbf{h}^T(\eta,\zeta)\mathbf{y} \\ z &= z_0 + \xi \mathbf{h}^T(\eta,\zeta)\mathbf{z} \end{aligned}$$

The following approximate description of the displacements u_i and the electric potential φ with the help of the shape functions **h** and unknown analytical nodal displacement functions $\mathbf{w}_h(\xi)$

$$\mathbf{w} = \left[u_1, u_2, u_3, \varphi\right]^T$$

$$\mathbf{w}_h\left(\xi,\eta,\zeta\right) = \mathbf{h}^T\left(\eta,\zeta\right)\mathbf{w}_h\left(\xi\right)$$

for the case of no electric or mechanical loads leads to

$$\int_{\xi=0}^{1} \delta\mathbf{w}(\xi)^T \left[\mathbf{E}_0\xi^2\mathbf{w}_h(\xi)_{,\xi\xi} + \left(2\mathbf{E}_0 + \mathbf{E}_1^T - \mathbf{E}_1\right)\xi\mathbf{w}_h(\xi)_{,\xi} + \left(\mathbf{E}_1^T - \mathbf{E}_2\right)\mathbf{w}_h(\xi)\right] d\xi$$
$$= \delta\mathbf{w}^T\left[\mathbf{E}_0\mathbf{w}_{h,\xi} + \mathbf{E}_1^T\mathbf{w}_h\right]$$

where

$$\mathbf{E}_0 = \int_\Gamma \mathbf{B}_1{}^T\mathbf{H}\mathbf{B}_1\left|\mathbf{J}\right| d\eta d\zeta \quad , \quad \mathbf{E}_1 = \int_\Gamma \mathbf{B}_2{}^T\mathbf{H}\mathbf{B}_1\left|\mathbf{J}\right| d\eta d\zeta \quad , \quad \mathbf{E}_2 = \int_\Gamma \mathbf{B}_2{}^T\mathbf{H}\mathbf{B}_2\left|\mathbf{J}\right| d\eta d\zeta$$

$$\mathbf{J} = \begin{pmatrix} \frac{\partial x}{\partial\xi} & \frac{\partial y}{\partial\xi} & \frac{\partial z}{\partial\xi} \\ \frac{\partial x}{\partial\eta} & \frac{\partial y}{\partial\eta} & \frac{\partial z}{\partial\eta} \\ \frac{\partial x}{\partial\zeta} & \frac{\partial y}{\partial\zeta} & \frac{\partial z}{\partial\zeta} \end{pmatrix} \quad , \quad \mathbf{H} = \begin{pmatrix} \mathbf{C} & -\mathbf{e}^T \\ \mathbf{e} & \boldsymbol{\epsilon} \end{pmatrix}$$

$$\mathbf{L} = \begin{pmatrix} \frac{\partial}{\partial x} & 0 & 0 & 0 & \frac{\partial}{\partial z} & \frac{\partial}{\partial y} & 0 & 0 & 0 \\ 0 & \frac{\partial}{\partial y} & 0 & \frac{\partial}{\partial z} & 0 & \frac{\partial}{\partial x} & 0 & 0 & 0 \\ 0 & 0 & \frac{\partial}{\partial z} & \frac{\partial}{\partial y} & \frac{\partial}{\partial x} & 0 & 0 & 0 & 0 \\ 0 & 0 & 0 & 0 & 0 & 0 & -\frac{\partial}{\partial x} & -\frac{\partial}{\partial y} & -\frac{\partial}{\partial z} \end{pmatrix}^T = \mathbf{L}_\xi\frac{\partial}{\partial\xi} + \mathbf{L}_\eta\frac{\partial}{\partial\eta} + \mathbf{L}_\zeta\frac{\partial}{\partial\zeta}$$

$$\mathbf{B}_1 = \mathbf{L}_\xi\mathbf{h}^T\left(\eta,\zeta\right) \quad , \quad \mathbf{B}_2 = \mathbf{L}_\eta\frac{\partial\mathbf{h}^T\left(\eta,\zeta\right)}{\partial\eta} + \mathbf{L}_\zeta\frac{\partial\mathbf{h}^T\left(\eta,\zeta\right)}{\partial\zeta}$$

The resulting Euler-Cauchy differential equations (together with some boundary conditions that are not relevant here)

$$\mathbf{E}_0\xi^2\mathbf{w}_{h,\xi\xi}+\left(2\mathbf{E}_0+\mathbf{E}_1^T-\mathbf{E}_1\right)\xi\mathbf{w}_{h,\xi}-\left(\mathbf{E}_2-\mathbf{E}_1^T\right)\mathbf{w}_h=0$$

have a solution known to be of the type

$$\mathbf{w}_h\left(\xi\right)=\xi^{\lambda_k}\mathbf{\Phi}_k$$

with a power law dependence in ξ where λ_k is a modal scaling factor in radial direction and the vector $\mathbf{\Phi}_k$ denotes the modal displacements at the boundary nodes. This leads to the quadratic eigenproblem

$$\left[\lambda_k^2\mathbf{E}_0+\lambda_k\left(\mathbf{E}_0+\mathbf{E}_1^T-\mathbf{E}_1\right)-(\mathbf{E}_2-\mathbf{E}_1^T)\right]\mathbf{\Phi}_k=0$$

that can be solved by standard methods for eigenproblems. The advantage of the scaled boundary finite element method for the determination of singularity orders is that the eigenvalues λ_k are automatically determined in the solution procedure with high accuracy, so the method provides very precise results for the singularity orders in the similarity center.

NUMERICAL EXAMPLES

The singularities considered were two-dimensional geometrical or material line singularities and combinations of both as well as their three-dimensional interaction at interaction points. As an example, a notch in an interface displayed in Fig. 3a will be discussed here since it includes all possible types of singularities. Two two-dimensional line singularities – the geometric discontinuity along the notch root Γ_1 and the material discontinuity along the interface Γ_2 – interact three-dimensionally in the interaction point *S*, the similarity center.

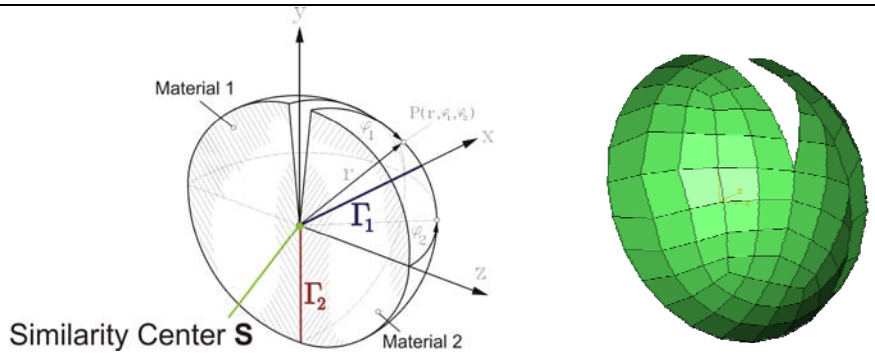

a. Geometry b. Mesh

Figure 3: Notch in an interface at a free edge. a. Geometry, b. Mesh.

The situation was analyzed for material combinations of 0°/θ° and ±θ° of unidirectional CFRP-material for orthotropic material with the material properties of T300/Epoxy and for a fictitious piezoelectric material with the mechanical properties of T300/Epoxy and the piezoelectrical and dielectrical properties of PZT-5A. The notch opening angle γ was chosen to vary from 0° (interface crack) to 90°.

The displayed mesh (see Fig. 3b) may be rather coarse, but this is indeed sufficient to determine precise singularity orders in the similarity center. Also not the entire boundary needs to be discretized since on the so-called side-faces and on the notch faces the method inherently presumes strong boundary conditions.

For the interface crack (γ=0°), the results for the singularity orders of the two two-dimensional singularities and the three-dimensional interaction point for a material combination of 0°/θ° of unidirectional CFRP-material are shown in Fig. 4 in the first line for orthotropic material with the material properties of T300/Epoxy and in the second line for a fictitious piezoelectric material with the mechanical properties of T300/Epoxy and the piezoelectrical and dielectrical properties of PZT-5A.

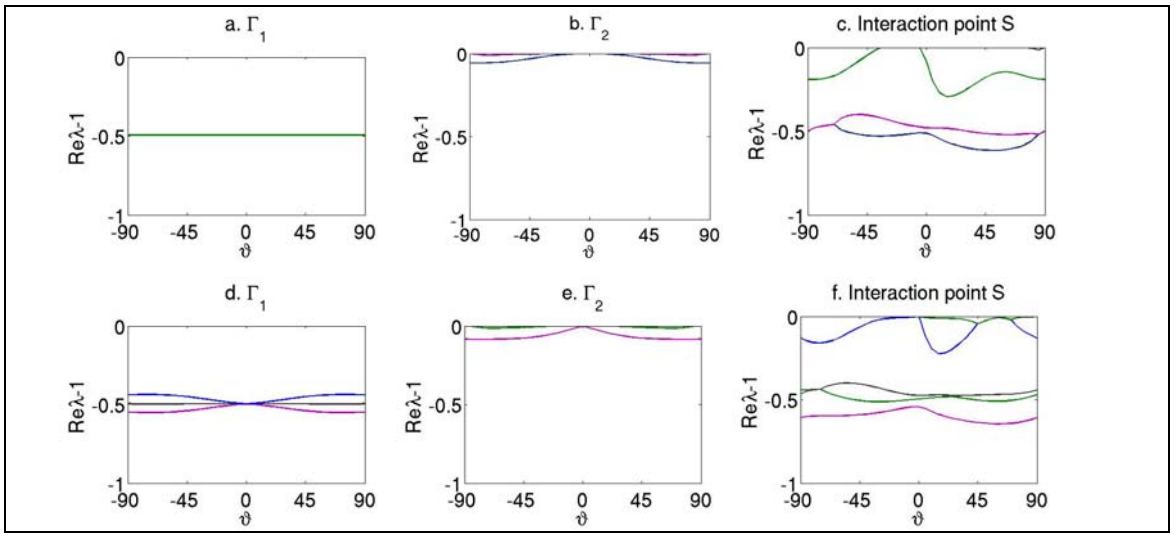

Figure 4: Singularity orders for the interface crack at a free edge for a 0°/θ° layup. a-c T300/Epoxy and d-f T300 Epoxy / PZT-5A.

It can be seen that for the pure mechanical case, Γ_1 yields the known crack singularity order, as expected. Comparing the results for this and the interface at a free edge with the singularity orders at the three-dimensional interaction point, it is evident that there is no clear relation between the singularity orders. In the three-dimensional case, real and complex orders occur and they are slightly stronger than the crack singularity order for some layups. The results for the piezoelectric materials are qualitatively similar to the ones of the orthotropic case. The results are slightly more complex in comparison. Again, there is no obvious relation between the singularity orders of the two two-dimensional singularities and the one of the three-dimensional interaction point.

Results for the singularity order at the interaction point for varying notch opening angles for a material combination of 0°/θ° of unidirectional CFRP-material for both materials are shown in Fig. 5.

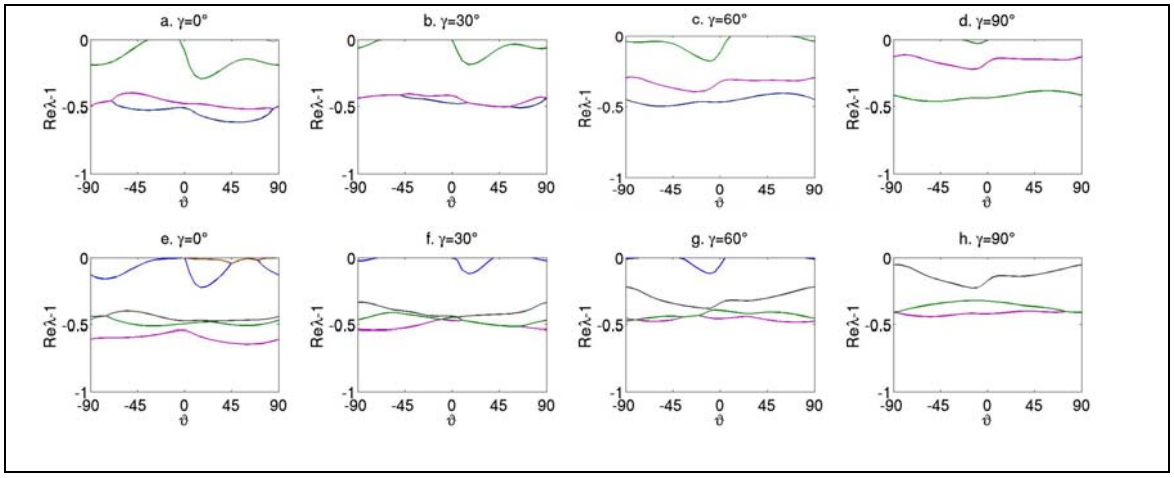

Figure 5: Singularity orders for the interface notch at a free edge with varying opening angles γ for a 0°/θ° layup. a-d T300/Epoxy and e-h T300 Epoxy / PZT-5A.

It can be seen that the singularity orders become less critical for both materials when the notch opening angle increases, as expected. For the opening angle of 30°, the strongest singularity order thus is already smaller than the known crack tip singularity. The results for the different angles resemble each other qualitatively, but where smaller angles have complex results these seem to split up into two real eigenvalues for larger opening angles. The results for the two-dimensional line singularities Γ_1 and Γ_2 are not shown for the other opening angles, but they also resemble the results for the interface crack with weaker singularity orders and the relation between the two-dimensional singularity orders and the singularity orders at the interaction point is equally complex. Comparing the results for both materials shows that again results for the piezoelectric material yield additional and stronger singularity orders.

The same situations were analyzed for a material combination of ±θ° of unidirectional CFRP-material. Fig. 6 shows the results for the singularity orders of the two two-dimensional singularities and the three-dimensional interaction point for the interface crack (γ=0°), again in the first line for T300/Epoxy and in the second line for the fictitious T300/Epoxy / PZT-5A material.

As for the other layup, it is noticeable that it seems impossible to deduce the three-dimensional singularity orders from the two-dimensional singularities in an easy manner. The results differ to some degree from the 0°/θ° results in that the largest singularity orders occur for different angles, the largest occurring singularity orders and the overall picture resemble the results for the other layup. All observations comparing results for the different materials still hold.

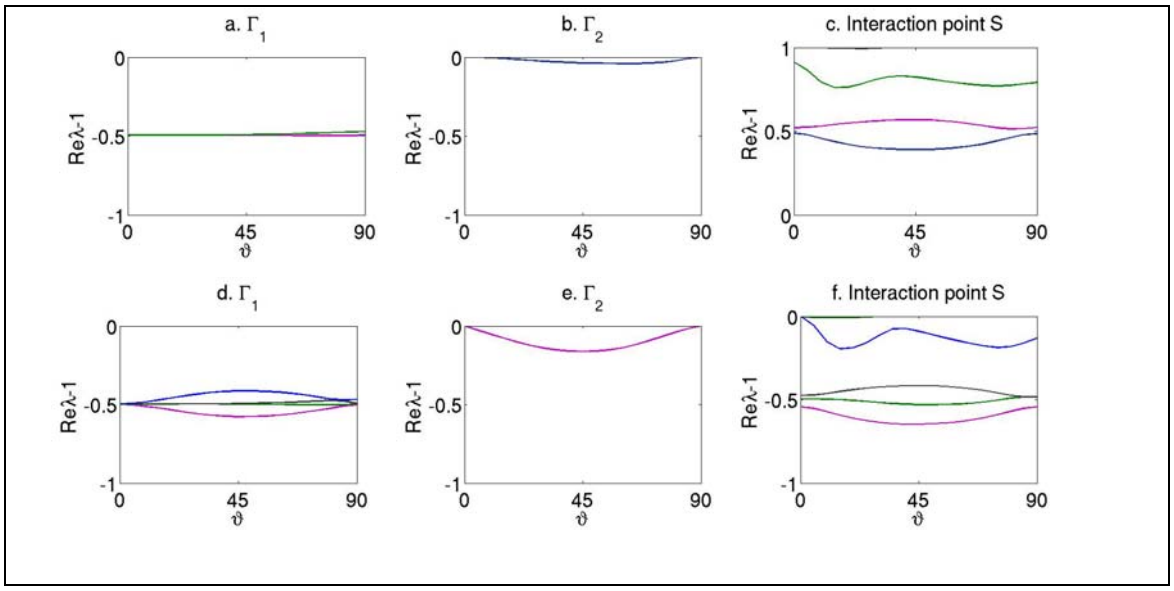

Figure 6: Singularity orders for the interface crack at a free edge for a ±θ° layup. a-c T300/Epoxy and d-f T300 Epoxy / PZT-5A.

Results for a material combination of ±θ° of unidirectional CFRP-material for varying notch opening angles for the singularity orders at the three-dimensional interaction point are shown in Fig. 7 for the same materials as above.

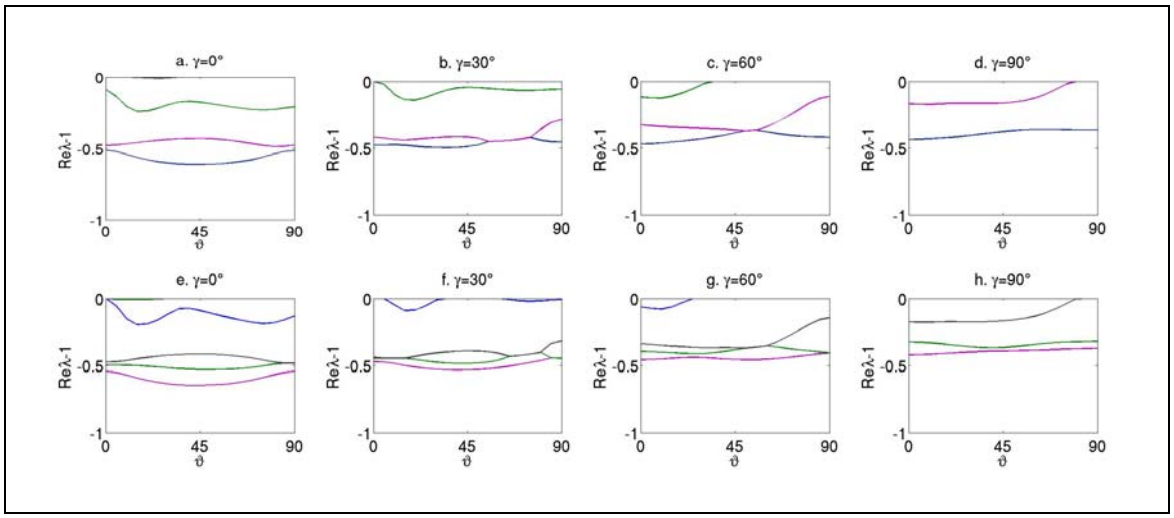

Figure 7: Singularity orders for the interface notch at a free edge with varying opening angles γ for a ±θ° layup. a-d T300/Epoxy and e-h T300 Epoxy / PZT-5A.

Again, the singularity orders decrease with increasing opening angles. As for the interface crack, the strongest singularity orders for all opening angles are comparable in size to the strongest singularity order for the 0°/θ° layup, but they do not necessarily occur for the same angle θ. The results overall resemble the results for the other layup. It also can be observed again that the type of singularity order is purely real for some

angles and complex for others. The results again show additional and stronger singularity orders for the piezoelectric material compared to the linear-elastic material.

In summary, the results show that singularity orders at three-dimensional interaction points are of a complex nature and can not be predicted easily from the corresponding two-dimensional singularities. Thus, there is a need for an analysis tool that can be used for such situations. By means of the scaled boundary finite element method, singularity orders can be determined with low effort. The singularity orders occurring can be real or complex, and they can be stronger than the known crack tip singularity. For the analyzed situations, piezoelectric materials yield additional and often stronger singularity orders than linear-elastic materials.

CONCLUSIONS

Stress singularity orders of various two- and three-dimensional situations can be determined by means of the scaled boundary finite element method. The effort generally is significantly lower than for standard methods. Complex results for singularity orders at three-dimensional interaction points show the need for an efficient tool for the analysis of such situations. The scaled boundary finite element method in the extended formulation for piezoelectric materials is such an efficient tool in elastic and piezoelectric multi-material systems.

ACKNOWLEDGEMENTS

This work has been performed under the financial support of 'Deutsche Forschungsgemeinschaft' under BE 1090/19-1, which is gratefully acknowledged.

References

1. **Wolf, J.P.; Song, Ch. (1996):** *Finite Element Modelling of Unbounded Media*. John Wiley & Sons, Chichester et al., England.
2. **Song, Ch.; Wolf, J.P.; (1997):** *The Scaled Boundary Finite-Element Method – alias Consistent Infinitesimal Finite-Element Cell Method – for Elastodynamics*. Computer Methods in Applied Mechanics and Engineering, 147:329-355.
3. **Artel, J.; Becker, W. (2006):** *Analysis of the free-edge effect in piezoelectric laminated plates by the scaled boundary finite element method*. Proceedings of the Eighth International Conference on Computational Structures Technology. Editors: B.H.V. Topping et al., Civil-Comp Press, CD-ROM.

Back to Programme *Back to Topic* *Next Paper*